

OPEN

Simultaneous detection and comprehensive analysis of HPV and microbiome status of a cervical liquid-based cytology sample using Nanopore MinION sequencing

Lili Quan^{1,4}, Ruyi Dong^{2,4}, Wenjuan Yang², Lanyou Chen², Jidong Lang², Jia Liu², Yu Song¹, Shuiqing Ma³, Jialiang Yang², Weiwei Wang², Bo Meng^{2*} & Geng Tian^{2*}

Human papillomavirus (HPV) is a major pathogen that causes cervical cancer and many other related diseases. HPV infection related cervical microbiome could be an induce factor of cervical cancer. However, it is uncommon to find a single test on the market that can simultaneously provide information on both HPV and the microbiome. Herein, a novel method was developed in this study to simultaneously detect HPV infection and microbiota composition promptly and accurately. It provides a new and simple way to detect vaginal pathogen situation and also provide valuable information for clinical diagnose. This approach combined multiplex PCR, which targeted both HPV16 E6E7 and full-length 16S rRNA, and Nanopore sequencing to generate enough information to understand the vagina condition of patients. One HPV positive liquid-based cytology (LBC) sample was sequenced and analyzed. After comparing with Illumina sequencing, the results from Nanopore showed a similar microbiome composition. An instant sequencing evaluation showed that 15 min sequencing is enough to identify the top 10 most abundant bacteria. Moreover, two HPV integration sites were identified and verified by Sanger sequencing. This approach has many potential applications in pathogen detection and can potentially aid in providing a more rapid clinical diagnosis.

More and more diseases have been shown to be associated with certain kinds of pathogens, including viruses and microbiomes^{1,2}. Microbes can contribute to digestive disorders (e.g., inflammatory bowel disease) and disease processes, such as an association with the degenerative lesions seen in Parkinson's disease, autism, depression³ and carcinogenesis⁴. Furthermore, in gastric cancer, the presence of *Helicobacter pylori* is considered a major contributing factor⁵; while *Fusobacterium* species are associated with colorectal cancer⁶. Moreover, various studies have indicated that an altered microbiome can be associated with disease^{7,8}. In HPV-positive women, cervicovaginal bacterial diversity is more complex relative to those who are HPV-negative^{9,10}, which indicates that there may be a direct relationship between the cervical microbiome and disease development. In addition to bacteria, viruses have also been shown to be causative agents in disease¹¹, with hepatitis B virus (HBV) associated with liver cancer, Epstein–Barr virus (EBV) associated with nasopharyngeal carcinoma, and human papilloma virus (HPV) associated with cervical cancer^{12,13}. So far, more and more studies found some virus integration status significantly correlated with disease development status, especially in HPV integration of cervical cancer¹⁴.

While cervical cancer is one of the most common female cancers worldwide, a detection method that provides an economical, convenient, and accurate clinical screening approach is still required. Current cervical cancer screening methods are usually based on high-risk HPV DNA or RNA genotyping, or on the detection of cytological and/or molecular changes in cervical cells via an immunostaining method, such as a Papanicolaou (Pap) smear¹⁵. Most of the screening methods just target HPV instead of microbiome. However, several studies have

¹Department of Gynaecology and Obstetrics, Sanmenxia Central Hospital of Henan University of Science and Technology, Sanmenxia, 472000, Henan, China. ²Geneis (Beijing) Co.Ltd, Beijing, 100102, China. ³Department of Gynaecology and Obstetrics, Peking Union Medical College Hospital, Beijing, 100730, China. ⁴These authors contributed equally: Lili Quan and Ruyi Dong. *email: mengb@geneis.cn; tiang@geneis.cn

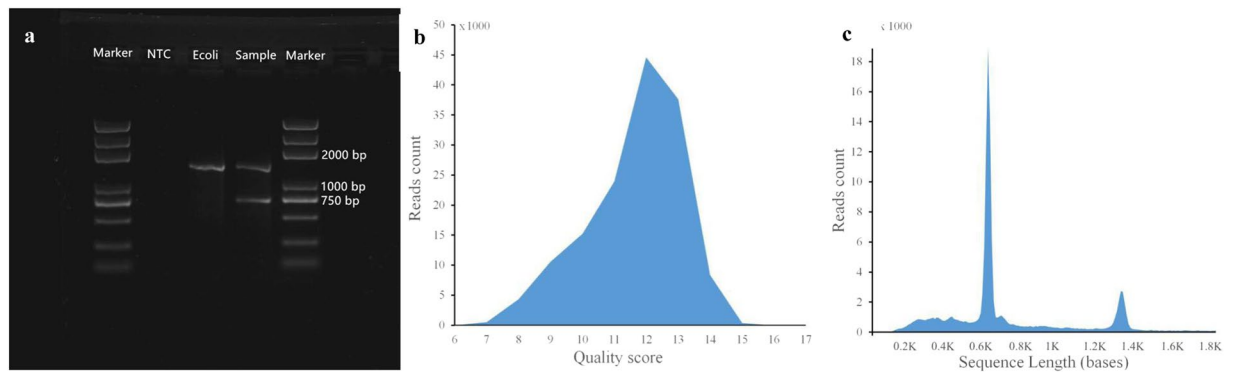


Figure 1. PCR products for Nanopore sequencing and sequencing quality and length distributions. (a) Agarose gel of multiplex PCR products, with the full-length gel presented in Supplementary Figure S2. Nanopore sequencing (b) Q-score and c. length distribution plots.

identified a correlation between a microbiome with HPV and cervical intraepithelial neoplasia (CIN) or cervical cancer¹⁶. One study identified a correlation between the cervical microbiota and CIN stage, with the co-effect of the microbiota and HPV determined to influence CIN risk¹⁷. *Fusobacteria*, including *Sneathia*, are the species most strongly correlated with HPV infections¹⁷. Additionally, another study showed that of the vaginal flora, *Lactobacillus* the dominant species can protect against other pathogens¹⁸. Other studies have suggested that during an HPV infection, the microbiome balance may be disrupted, with other species, like *Gardnerella vaginalis* and *Chlamydia trachomatis*, meanwhile, *Lactobacillus gasseri* and other anaerobic species becoming more prevalent^{9,19,20}. This vaginal microbiome alteration may then affect pathogenesis by affecting immunity or increasing the growth of pathogenic strains²¹. With more and more studies revealing that microbiome alterations can serve as disease diagnostic indicators, with the potential to be used as early screening triage markers for cervical cancer²², and aid in the development of analytical methods for detecting the microbiome, such as 16S rRNA sequencing, they have gained interest²³.

The 16S rRNA gene contains conserved and variable regions that can be used to differentiate microorganisms within the same sample, with the V1 and V9 regions commonly amplified via PCR^{24,25}. However, studies utilizing next-generation sequencing technology have predominantly used the V4 or V3V4 regions for identification^{26–28}, while other studies have used other regions^{29,30}. When determining which region to utilize, some regions provide more information when utilizing short sequencing reads³¹, while others are more informative when a taxonomic approach is employed³²; therefore, some researchers utilize a full-length 16S rRNA sequence for analysis. With the development of third-generation sequencing technology, it is now possible to completely sequence a full-length gene with a maximum read length up to 2 Mb³³. In one study, this technology was utilized to sequence the 16S rRNA gene and showed that accurate results can be obtained when compared with Illumina sequencing results³⁴. However, this approach is not as portable as employing a Nanopore in the application. In a study evaluating mouse full-length 16S rRNA sequencing obtained using Nanopore or Illumina, with the V3V4 region utilized, the Nanopore sequencing provided better annotation results at the specie level³⁵. However, due to the relatively high error rate that is associated with Nanopore sequencing, its application in clinical studies is still very limited.

Nanopore sequencing has been successfully employed in genome assembly, structure variation detection, real-time sequencing of pathogenic microbes, antibiotic resistance profile identification, and the detection and identification of viral or bacterial pathogens in various clinical samples^{36–40}; thus, implementing this approach in clinic pathogen and microbiome studies is of interest. Additionally, some studies have identified both viral and bacterial species accurately when utilizing Nanopore amplicon sequencing^{41,42}, with NanoAmpli-Seq successfully applied for full-length 16S rRNA gene sequencing and shown to provide a high accuracy⁴³. However, while accurate sequencing is an advantage, the library construction process is relatively complex and requires extra data analysis steps and would not be able to provide the quick results that the area expected in a clinical setting.

HPV detection has been clinically proven as imperative for early cervical cancer detection, and the integration status of HPV in patient DNA has also shown to be correlated with cervical carcinogenesis. Studies have shown that the integration sites are distributed throughout the genome, including integration hotspots at 3q28, 17q21, 13q22.1, 8q24.21, and 4q13.3, and are often induced by HPV E1, E6, or E7 proteins⁴⁴. Thus, the ability to collect information pertaining to the HPV infection, HPV integration status, and microbiome status simultaneously would provide valuable clinic information for screening and prevention.

Herein, a novel process was developed to enable the sequencing of an HPV16 E6E7 fragment and a full-length 16S rDNA simultaneously by using multiplex PCR followed by Nanopore sequencing. One clinical sample was examined and shown to be HPV16 positive. The HPV integration sites were identified using a probe capture method, and sequencing was performed using an Illumina sequencer.

Results

Nanopore sequencing of multiplex HPV E6E7 and full-length 16S rRNA PCR products. Full-length 16S rRNA and HPV16 E6E7 amplicons were obtained as described above, with 750 bp (HPV E6E7) and 1,500 bp (16S rRNA) fragments obtained (Fig. 1a). A Nanopore sequencing library was constructed and sequenced using a Nanopore sequencer. The sequencing generated 189,511 reads from 977 pores. To obtain

Platform	Raw reads	Quality filtered reads ($\geq Q20$)	Pass 1D reads	Joined reads	Length (bp)			Sequence quality Scores		
					Min	Mean	Max	Min	Mean	Max
Illumina	1,453,612	1,284,004(88.35%)	/	427,886 (58.88%)	151	249.2	292	19	32.78	35
Nanopore	189,511	/	145,605(76.8%) (120.7M)	/	88	854	15,068	7	12.65	17

Table 1. Illumina and Nanopore sequencing data statistics.

high-quality reads, the raw data were filtered using the Metrichore 1D base calling program to improve the mean quality score and total read accuracy. A total of 145,605 reads (76.8%; passes 1D reads) were retained with quality scores ranging from 7 to 17, with a mean value of 12.65 (Fig. 1b, Table 1). The read lengths ranged from 88 to 15,068 bp, with a mean read length of 854 bp (Fig. 1c, Table 1).

HPV infection and microbiome analysis of Nanopore results. Nanopore sequencing results were analyzed according to the pipeline described in Supplementary Fig. S1 and then evaluated using LAST (<http://lastweb.cbrc.jp>), with the HPV genome and NCBI 16S ribosomal RNA (Bacteria and Archaea) databases queried following quality score ($Q \geq 7$) filtering. The results identified 71,276 reads that matched the HPV16 genome, 48.9% of the passed 1D reads, thus indicating a high amplification efficiency and a high virus load in this sample. Additionally, 17,826 reads matched 16S rRNA sequences, 12.24% of the passed 1D reads. The remaining unmatched reads totaled 56,503 (Supplementary Table S1).

To analyze the microbiome data more accurately, QIIME (Quantitative Insights into Microbial Ecology) was used to assign taxonomy annotations at all classification levels from phylum to genus (Supplementary Tables S2 and S3). At the phylum level, four phyla were identified, including Firmicutes, Proteobacteria, Bacteroidetes, and Actinobacteria, with Firmicutes being the most abundant (98.9%). Seven classes were identified, including Bacilli, Clostridia, Bacteroidia, Actinobacteria, Alphaproteobacteria, Betaproteobacteria, and Gammaproteobacteria, with Bacilli being the most abundant (96.6%). Additionally, 8 orders and 15 families were identified, with Lactobacillales and Enterococcaceae being the two most abundant families among those tested. In total, 21 genera were identified, with *Enterococcus* being the most abundant (94.1%). Bacteria associated with bacterial vaginosis (BV)⁴⁵ were also examined, and six genera were identified, including *Bacteroides*, *Prevotella*, *Enterococcus*, *Streptococcus*, *Staphylococcus*, and *Peptostreptococcus* (Supplementary Table S4).

Taxonomic annotation comparison between the 16S rRNA Illumina V4 results and the Nanopore 16S full-length results. To evaluate the accuracy of the Nanopore results, the 16S rRNA V4 region of the same sample was amplified by PCR and sequenced using an Illumina next-generation sequencer. In total, 1,453,612 raw reads (219.5 M raw bases) and 1,453,363 clean reads (217.3 Mb) were obtained when using the Illumina sequencing platform (Table 1), with 1,284,004 (88.35%) reads retained after quality filtering. A total of 427,886 (58.88%) sequencing reads were then joined, with lengths between 151 bp and 292 bp and an average length of 249 bp. The quality score range was from 19 to 35, with an average of 32. Approximately 4% (27,123) of the sequencing reads were retained for further microbial community analysis (Table 1).

The paired passing filter reads were classified using QIIME and were grouped into 7 phyla, 13 classes, 16 orders, 32 families, 50 genera, and 7 species. The annotation results from the Illumina platform were then compared with the Nanopore results at the phylum, class, order, and genus levels (Fig. 2, Supplementary Tables S2 and S3). When examining the bacteria, both platforms identified 4 phyla, 7 classes, 10 orders, 15 families, and 20 genera (Supplementary Tables S2 and S3). Several conclusions can be drawn from the results: (1) both of the platforms identified p_Firmicutes, c_Bacilli, o_Lactobacillales, f_Enterococcaceae, and g_Enterococcus as a significantly dominant population, with 85% and 94% relative abundances in the Illumina and Nanopore results, respectively. (2) The Illumina results have more unique taxonomic units than the Nanopore results, with the Nanopore results having only one unique genus (*Vagococcus*, 0.035%), while the Illumina results had multiple at the phylum (3/7), order (6/16), class (6/13), family (18/33), and genus (31/51) levels. These findings suggest that the Illumina platform is more sensitive and can detect more bacterial categories when compared with Nanopore. The difference could also be attributed to Illumina generating larger datasets with more sequencing depth or differences in the QIIME pipeline for short and long sequence reads. (3) While Illumina identified more unique taxonomic units, the two platforms generated an overlapping bacteria list for each level, with orders having an 80% overlap and belonging to the top 10 orders, while other units were all associated with the highest units (Supplementary Table S2). Based on the calculated high abundance taxonomic unit results, there is only one unique Illumina units in the top 5 phyla, 3 in the top 10 classes, 2 in the top 10 orders, and none in the top 15 families or top 20 genera. These findings indicate that most of the unique units identified by using the Illumina V4 method are at a low abundance and may be attributed to an experimental or analytical bias. (4) Without performing any additional analytics, the identified taxonomic unit results when comparing the Nanopore and Illumina results show a strong concordance among the most abundant bacteria at each level (Supplementary Table S3). When comparing the two platforms, the Spearman's rank correlation results gave a 0.9265616 at the phylum level, 0.8796751 at the class level, 0.8409996 at the order level, 0.7095144 at the family level, and 0.6583039 at the genus level. In conclusion, the Nanopore platform detected the dominant *Enterococcus* genus and 20 other genera that overlap with the Illumina V4 results. Furthermore, when examining the 16S rRNA, they were 100% consistent at the genus level, which strongly suggests that the Nanopore platform can provide acceptable results by sequencing a full-length 16S rRNA. (5) BV-related bacteria within the Illumina results were examined, and 10 genera were

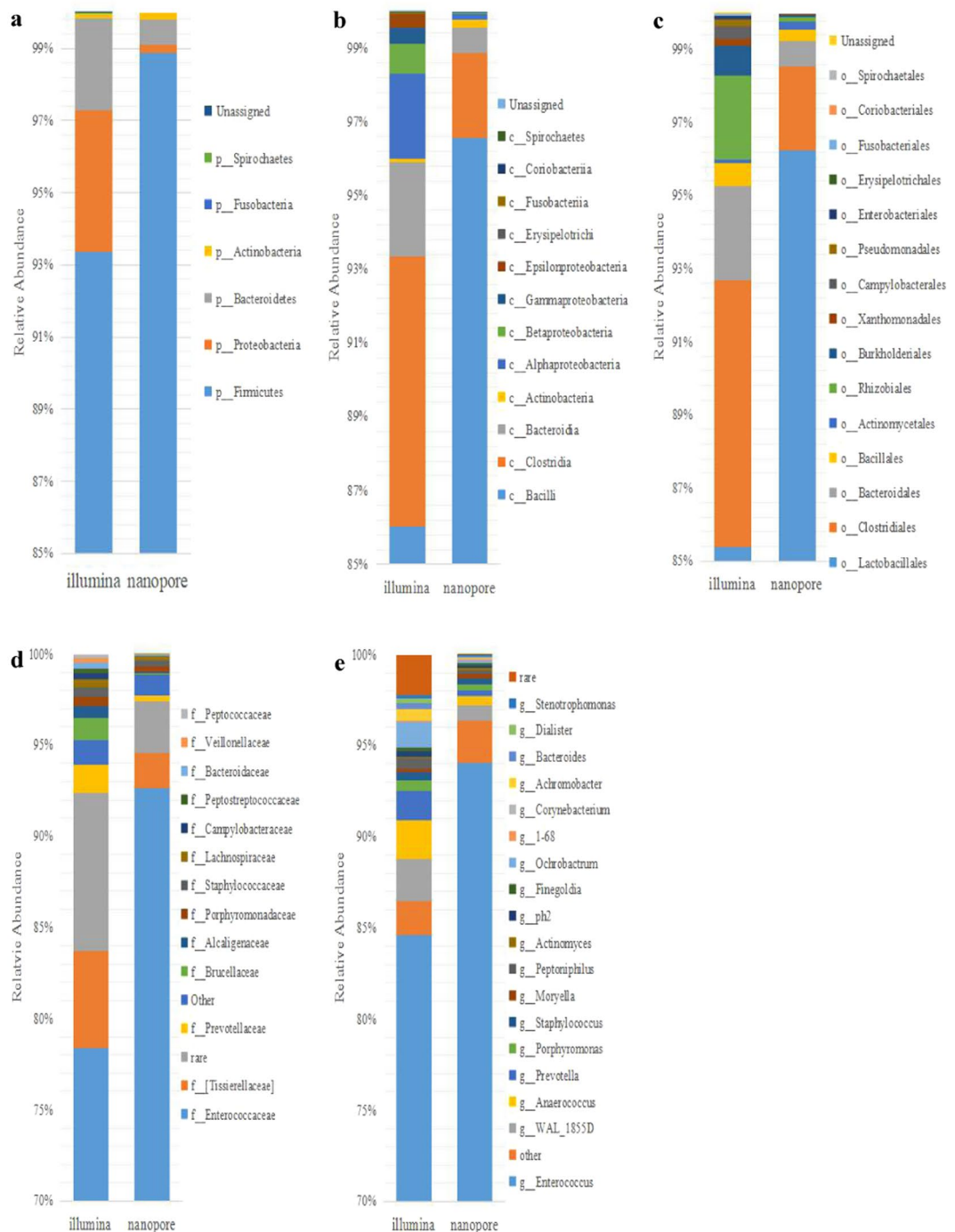


Figure 2. Comparison between the taxonomic profiles obtained from two different sequencing platforms at different taxonomic levels (phylum to genus). **(a)** phylum level, **(b)** class level, **(c)** order level, **(d)** family level, and **(e)** genus level.

identified, with *Bacteroides*, *Prevotella*, *Enterococcus*, *Streptococcus*, *Staphylococcus*, and *Peptostreptococcus* also identified by the Nanopore platform (Supplementary Table S4).

Specie annotation result comparisons when using different analytical methods and databases. Nanopore results were further annotated at the specie level using QIIME and LAST, with the GreenGenes database, and the methods were named QIIME_GreenGenes and LAST_GreenGenes. The results annotated 5,574 reads to 23 genera (reads ≥ 2), with only 3 species clearly annotated using the QIIME_GreenGenes method, while the remaining 20 genera could not be annotated using this method (Fig. 3a, Supplementary Tables S5 and S6). The LAST_GreenGenes method identified 53 genera (reads ≥ 2) and annotated 19 species, with only 6 species of the overlapped genera identified. Since most of the genera were without specific

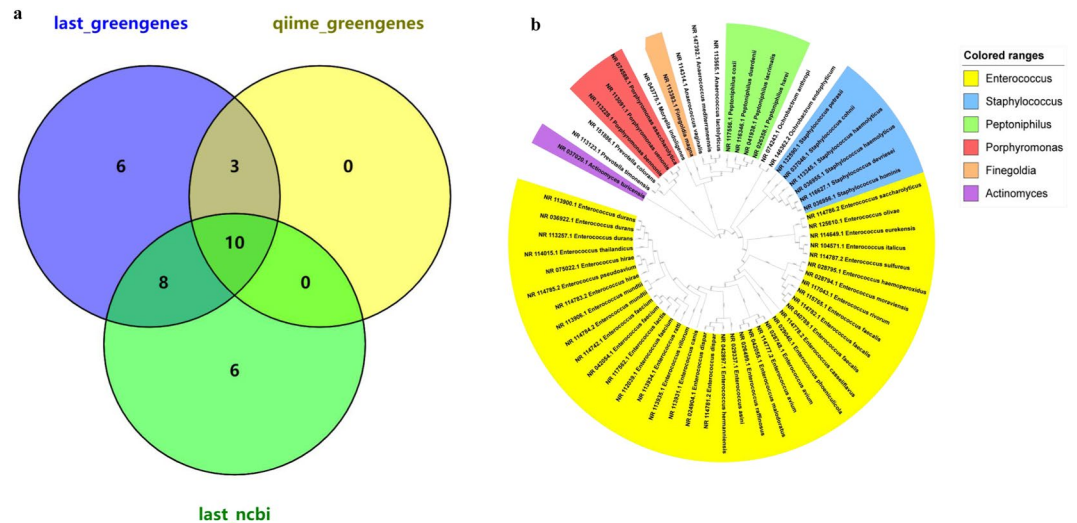


Figure 3. Nanopore 16S rRNA results when overlapping different databases. **(a)** A venn diagram displaying the findings for different databases at the genus level. **(b)** A phylogenetic tree of species annotated using the LAST_NCBI method.

Overlapped Genus	Number of Identified Species		
	QIIME_greenenes	Last_greenenes	Last_NCBI
g_Actinomyces	0	0	1
g_Anaerococcus	0	0	7
g_Enterococcus	1	2	33
g_Finegoldia	0	0	1
g_Moryella	1	0	1
g_Ochrobactrum	0	0	3
g_Peptoniphilus	0	0	8
g_Porphyromonas	0	0	4
g_Prevotella	0	0	5
g_Staphylococcus	1	4	7
Total	3	6	70

Table 2. Summary of the species that were identified when utilizing the 10 genera that were commonly identified using three different analytical methods.

specie annotations, the LAST_NCBI database was utilized to attempt to obtain better annotation results. By using this method, all 127 genera (reads ≥ 2) were annotated with at least one specific species. Overall, 197 specific species were found, including 70 species belonging to the 10 overlapped genera (Table 2, Supplementary Tables S5 and S6). When comparing all three of the analytical methods, only two genera, *Enterococcus* and *Staphylococcus*, had specie annotations in all three methods. When using the LAST_NCBI method, 7 of the 10 overlapped genera were identified in multiple species, especially *Enterococcus*, with over 90% of the identified reads annotated to 33 specific species. Another genus, *Peptoniphilus*, was classified to eight specific species (Supplementary Tables S5 and S6). Overall, these comparison results clearly show that a significant improvement in specie annotations can be obtained when using the LAST_NCBI analysis method.

These bacterial strains (reads ≥ 5) were annotated using the LAST_NCBI method and were used to construct a phylogenetic tree (Fig. 3b). The phylogenetic tree showed that the strains classified into five separate groups, with *Actinomyces* in a separate outside branch. *Enterococcus* was the most abundant genus, with 27 different species (reads ≥ 5) and 37 strains, and comprised the first group. The second and third groups included *Staphylococcus* (6 species) and *Ochrobactrum* (2 species; reads ≥ 5). *Anaerococcus* (n = 3), *Finegoldia* (n = 1), *Moryella* (n = 1) and *Peptoniphilus* (n = 4) strains all comprised the fourth group. The fifth group included two genera, *Porphyromonas* (n = 3) and *Prevotella* (n = 2).

Rapid clinical sample pathogen detection via Nanopore MinION. To evaluate the minimum sequencing time required for both HPV16 and full microbiota detection, different percentages (5%, 10%, 15%, 20%, 25%, or 30%) of the total sequencing reads were extracted four times, and the microbiota composition was compared with the full sequencing results (Table 3 and Supplementary Tables S7 and S8). The results showed that

Ratio	Estimated sequencing time (min)	Extracted reads (avg.)	16S (avg.)	HPV (avg.)	TOP10 bacteria reads (avg.)	TOP10 bacteria numbers (avg.) (reads > 4)	Correlation coefficient with all	P-value
5%	15	4,459	919	3,540	859	7	0.999	0.109
10%	30	8,851	1,768	7,083	1,661	9	0.999	0.109
15%	45	13,332	2,668	10,664	2,503	10	0.999	0.109
20%	60	17,801	3,606	14,195	3,384	10	0.999	0.109
25%	75	22,295	4,432	17,863	4,141	10	0.999	0.109
30%	90	26,780	5,362	21,418	5,035	10	0.999	0.109
all	300	89,102	17,826	71,276	16,672	10	1	/

Table 3. Summary results from different extracted Nanopore sequencing reads.

HPVtype	HPV integration location	Chromosome	Chr. integration location	HPV gene	Human gene	Number of identified
HPV16	4,687	2	142,193,255	L2	<i>LRP1B</i>	224
HPV16	4,721	2	142,272,444	L2	<i>LRP1B</i>	20
HPV16	908	2	142,175,473	E1	<i>LRP1B</i>	10
HPV16	1,458	2	142,265,838	E1	<i>LRP1B</i>	170

Table 4. *LRP1B* integration sites identified using HPVDetector (n > 10).

when extracting as few as 4,459 reads from the total sequenced reads, the Nanopore platform can detect the top 10 abundant species that were identified when utilizing all of the sequencing results. Statistical and correlation coefficient analyses showed that there is no significant difference when using a subset of the reads or the total number of reads in terms of identifying bacterial species. These findings indicate that using this Nanopore amplicon library sequencing method can enable both HPV and microbiota species to be identified in as short as about 15 min when using this sequencing process. Overall, from the point of DNA extraction through sequencing, with sequencing times varying from 10 min to several hours, the process takes an average of 6 h. However, while the combination of multiplex PCR and Nanopore sequencing to detect HPV virus and other potential microbial pathogens in clinical samples looks promising, further examination into the applicability of this rapid detection method is required.

HPV integration site detection and verification. HPV integration sequences were further enriched and sequenced by using probe capture and Illumina sequencing. HPVDetector was used to analyze the integration sites and the results identified a number of integrations, with HPV16 E1 and L2 (NC_001526.4) significantly enriched in *LRP1B* on chromosome 2 within the human genome (GRCh37/hg19). The integration site distributions are shown in Supplementary Tables S9 and S10, and the integration sites located within 200 bp are recognized as one. In the *LRP1B* gene, 4 sites were found to be integrated with HPV16 E1 or L2, with at least 10 sites identified by HPVDetector (Table 4). The location of HPV and *LRP1B* was calculated based on the average values of the merged locations. Overall, a total of 461 potential HPV integration sites were discovered in 22 different genes (Supplementary Tables S9 and S10). These identified high integration sites were then validated using Sanger sequencing, and a total of two unique HPV16 integration sites in the *LRP1B* gene were verified (Fig. 4). Therefore, these findings confirm that this patient is not only HPV16 infected but also HPV16 integrated.

Discussion

The human microbiota is a complex ecosystem of diverse microorganisms consisting of bacteria, fungi, and viruses that predominantly reside in epidermal and mucosal regions across the body²³. To investigate the role of microbiota in human health, including microbiota-host interactions and microbiota associations with diseases, especially cancers^{46,47}, several methods have been employed for determining the microbial community composition from clinical samples⁴⁸. Conventionally, microbial diversity analyses have focused on the V4 hypervariable region of the 16S rRNA gene and have utilized the Illumina platform⁴⁹. However, the short sequencing reads obtained when using this platform often limit the microbial composition analysis at the species level due to a high similarity between the 16S rRNA amplicon sequences³⁵. To overcome this limitation, obtaining a full-length 16S rRNA gene sequence using the Nanopore MinION sequencing platform has been explored^{29,50,51}. In this study, a new strategy enabling the simultaneous analysis of an HPV infection and microbiomes using Nanopore sequencing was explored and shown to be effective.

Other studies have attempted to perform a more rapid Nanopore data analysis, with one study establishing a relatively simple workflow for rapid bacterial identification via MinION™ sequencing using a mock bacteria community instead of using a real environmental or clinical sample⁵². Furthermore, another study established an amplicon sequencing (AmpSeq) workflow for predicting Newcastle disease viral virulence and genotype and was able to correctly identify NDV genotypes in all serial dilutions with an accuracy of 98.37%~100% after only 7 min of sequencing⁵³. Additionally, another study developed a portable system for analyzing 16S rRNA using a Nanopore sequencer and was able to detect 20 bacteria in a mock sample after 5 min of sequencing, with the results being consistent with those obtained after 4 h of sequencing⁵⁴. Herein, data analysis and sequencing were

The Nanopore MinION sequencer has the advantage of being portable and cost effective^{55,57}. While the error rate of this platform is still under debate, it shows clinical applicability for use as a rapid detection system for viral or bacterial detection^{50,58–60}. Various studies have shown that utilizing certain data correction methods can significantly minimize the error rate. For example, CANU⁶¹ and MECAT⁶² can be used to do self-correction with Nanopore sequencing data or hybrid Illumina/Nanopore datasets, with this improved accuracy potentially broadening the applicability of this technology. Furthermore, some studies have even used this platform to accurately sequence antibiotic resistance sites⁶³. Herein, only LAST was utilized to analyze and annotate the Nanopore sequencing. While the exact error rate of the sequencing data was not determined, the results showed a high degree of comparability with the Illumina results. One major reason could be that the most abundant microbe was present in several genera, thus providing enough coverage of the genus to annotate. In addition to the most abundant genera, the other genera with a relative abundance of about 0.03% could still be detected. These findings indicate that this method is feasible for detecting low abundance bacteria in clinic samples. However, further studies need to establish the lowest limit of detection.

The liquid-based cytology sample used in this study represents a huge population of clinical resources that are routinely collected yearly. The main screening methods for cervical cancer are Papanicolaou (pap) smear, cervical liquid-based cytology, cervicography, cervical biopsy or HPV testing^{64–66}. The liquid-based cytology (LBC) is widely used in the detection of gynecological specimens, vaginal or uterine, for the screening or diagnosis of cervical epithelial lesions⁶⁷. Recent reports have increasingly focused on utilizing LBC in combination with HPV-DNA detection when screening for cervical cancer to improve accuracy and sensitivity in pathogen detection^{19,21,67,68}. Studies examining correlations between the cervical BV-related microbiome, HPV screening and HPV infection, and cervical microbiome alterations have shown that there is a certain correlation between an HPV infection and the occurrence of cervicitis, cervical lesions, and cervical cancer^{69–71}, while the vaginal microbiome plays a functional role in the persistence or regression of HPV infections and the occurrence of cervical cancer^{8,72}. Lee *et al.* showed that *Fusobacteria*, including *Sneathia* spp., can serve as a possible HPV microbiological marker⁷³. Furthermore, another study reported that the vaginal microbiome in high-grade (HSIL) samples is characterized by higher levels of *Sneathia sanguinegens* ($P < 0.01$), *Anaerococcus tetradius* ($P < 0.05$), and *Peptostreptococcus anaerobius* ($P < 0.05$), while lower levels are characterized by *Lactobacillus jensenii* ($P < 0.01$) when compared to intra-epithelial lesions (LSIL)⁸. Therefore, collecting all of the information for every woman as early as possible so the microbiota associated with healthy and early disease states can be better characterized is essential to aid in disease prevention or treatment.

In one study, a similar type of sample was used, and the microbiome was identified using a proteomic approach, but only limited information could be detected⁷⁴. Herein, a method based on molecular nucleotide information was utilized to define the microbiome information by successfully analyzing a liquid-based cytology sample and identifying an HPV infection and bacterial content. Although only one sample was used in this study, the findings support its future applicability of this method to define HPV and its types and infections. In this study, only one primer was designed, HPV16 E6E7, but there are tens of high-risk HPV types that exist. Of these, some types are prevalent in human samples, including cervical samples, head and neck samples, and more than ten kinds of human organ-related samples. Furthermore, full-length 16S rRNA sequencing can promptly provide a patient pathogen profile to aid in performing a clinic diagnose, including applications in bacteria discovery in meningitis⁷⁵, liver abscess⁴⁰, and empyema⁵⁴. Thus, this workflow developed to detect HPV and the microbiome can be expanded to study other clinic samples and can aid in clinic diagnostic applications outside of cervical cancer.

In cervical carcinogenesis, HPV integrates into the host genome following a break in the E2 gene, which has been described as the main repressor of the expression of the E6 and E7 oncogenes and is a key genetic event in cervical carcinogenesis^{9,16,17,76}. The level of HPV integration was reported to be positively correlated with cervical intraepithelial neoplasia (CIN) grades and has even been proposed as a marker for disease progression^{77,78}. Moreover, another study found that HPV integration in *LRP1B* decreases its protein expression⁷⁰. HPV integration in *LRP1B* has also been found in oropharyngeal squamous cell samples⁷⁹. This study identified and verified two major HPV16 integrations (E1 and L2) in the human *LRP1B* gene. While many other integration sites were sequenced by the next-generation sequence, Sanger sequencing can only detect high abundance sequences due to the limitation of the technique. Thus, the other identified integration sites will have to be verified using other more sensitive molecular detection methods that are able to verify low abundance sequences in the future. Nevertheless, these results show correlations with previous studies. This study showed that this patient was not only infected with HPV16, but the virus was also integrated, thus indicating a potentially carcinogenic attribute to cervical cancer which requires further attention. Overall, identifying HPV integration breakpoints in the human genome and elucidating the mechanisms of integration can enable a better understanding of HPV-induced cervical carcinogenesis. Furthermore, it is also beneficial to discover novel and more specific biomarkers for diagnosis and treatment.

At present, this study detected HPV-DNA within a LBC sample following multiplex PCR and Illumina and Nanopore sequencing. Moreover, both the HPV and microbiota were characterized by using multiplex PCR technology using MinION. This not only shows the relationship between HPV integration and cervical cancer progression but also reveals a correlation between the bacterial community and the HPV integration status, which can aid in the early diagnosis and treatment of cervical cancer.

Conclusions

Herein, a novel approach was developed to enable the simultaneously detection of HPV and bacteria in a human LBC sample using Nanopore sequencing. This approach expands the pathogen detection potential of the Nanopore platform and offers rapid results that are desirable in a clinical setting. This study also showed that Nanopore sequencing of full-length 16S rRNA can provide comparable microbiota results to those obtained when utilizing the Illumina V4 sequencing method, with the top most abundant genera consistent between platforms.

Additionally, four HPV16 L2 or E1 integration sites within the *LRP1B* gene were identified, with two of them verified using Sanger sequencing. A deep analysis was performed to examine HPV infection and microbiome features associated with the examined patient sample to establish a broad potential application for HPV and microbiome analysis in a clinical setting. This approach can potentially be utilized as a diagnostic tool or can be potentially be utilized in other research and application areas.

Material and Methods

Sample information. Exfoliated cervical epithelial cell samples were collected and diagnosed as negative for intraepithelial lesions or malignancy (NILM) using the LBC. The sample used in this study was collected at the Sanmenxia Central Hospital, Henan Province, China, and the patient was 66 years old. The sample was collected for an HPV screening test, and the residual sample was used for this study. The sample was found to be HPV16 positive using a fluorescent HPV Genotyping kit (Bioperfectus Technologies, Jiangsu, China). This study was approved by the Medical Ethics Committee of Sanmenxia Central Hospital, Henan, China (Consent Number PROT No.36 [2018]). All experiments were performed in accordance with relevant guidelines and regulations and informed consent was obtained from the patient.

Genomic DNA extraction. Genomic DNA (gDNA) was extracted from exfoliated cervical epithelial cells using a TIANamp Micro DNA Kit (Tiangen, Beijing, China) according to the manufacturer's protocols. Briefly, samples were collected and stored in 1.5 ml sterilized tubes at 4 °C. A cell pellet was then formed following centrifugation at 5,000 rpm for 5 min and the DNA was extracted. The double-stranded (ds) DNA concentration was quantified using a Qubit dsDNA HS Assay Kit and Nanodrop 2000 (Thermo Fisher Scientific, Inc., Waltham, MA, USA).

Amplification of 16S V4 and Illumina sequencing library construction. The isolated gDNA was used as a template to amplify the V4 hypervariable region of the 16S rRNA gene⁸⁰. PCR was performed in a total volume of 20 µL and contained 10 µL KAPA HiFi HotStart Ready Mix (KAPA Biosystems, Wilmington, MA, USA), 0.5 µL each primer (10 nM), and 20 ng gDNA. Reactions were initially heated to 94 °C for 3 min, followed by 5 cycles at 94 °C for 30 s, 45 °C for 20 s, and 65 °C for 30 s; 10 cycles at 94 °C for 30 s, 50 °C for 30 s, and 72 °C for 30 s; and 15 cycles at 94 °C for 30 s, 55 °C for 30 s, and 72 °C for 30 s. Reactions were completed at 72 °C for 5 min.

Amplified PCR products were purified using 1.6× Agencourt AMPure XP beads (BeckmanCoulter Genomics, Brea, CA, USA) and then verified using 2% agarose gel electrophoresis. The purified DNA was then used to construct Illumina libraries using the NEBNext[®] UltraII[™] DNA Library Prep Kit for Illumina[®] (E7370L; New England Biolabs, Ipswich, MA, USA) and NEBNext[®] Multiplex Oligos for Illumina[®] (E6609L; NEB) according to the manufacturer's instructions. The generated library was quantified using a Qubit dsDNA HS Assay Kit (Thermo Fisher Scientific) with a Qubit 3.0 fluorometer (Invitrogen) and qualified using an Agilent 2100 TapeStation (Agilent Technologies, Santa Clara, CA, USA). The libraries were paired-end (2 × 150 bp) sequenced using an Illumina NextSeq Mid Output platform with a NextSeq 500/550 Mid Output v2 kit (300 cycles) in rapid run mode according to standard Illumina sequencing protocols.

HPV and 16S rRNA amplification. The gDNA obtained from the LBC was used as a template and the full-length 16S gene was amplified using specific primers (S-D-bact-0008-c-S20 and S-D-bact-1391-a-A-17)²⁶, while simultaneously amplifying the HPV16 genome using HPV16 E6E7 specific primers (NC_001526.2; Supplementary Table S11). The PCR reaction was carried out in a total volume of 25 µL containing 12.5 µL 2x GC buffer I (TaKaRa, Shiga, Japan), 2 µL dNTPs (2.5 µM), 0.5 µL each of forward and reverse primer (10 µM), 0.5 µL LA Taq[®] with GC Buffer (TaKaRa; 125 U), 2 µL template DNA (20 ng), and 1.0 µL nuclease-free water (not DEPC-treated). The amplification conditions were as follows: 4 min at 94 °C; then 30 cycles at 94 °C for 30 s, 50 °C for 40 s for annealing, and 72 °C for 90 s; and a final 72 °C for 15 min. PCR products were verified via gel electrophoresis and cleaned-up with AMPure XP beads (Beckman Coulter, Miami, FL, USA). Amplicons were quantified using a Qubit 3.0 fluorometer (Life Technologies, Carlsbad, CA, USA), and 1000 ng of the purified amplicon was used to generate a MinION library.

Amplicon DNA library preparation and ONT sequencing. The amplicons were prepped using a Ligation Sequencing kit (SQK-LSK108; Oxford Nanopore Technologies) with Native Barcoding Expansion (EXP-NBD103; ONT), according to the manufacturer's protocol for 1D Native barcoding gDNA. The prepared library (12 µL at ~158 ng) was then combined with 35 µL of running buffer containing Fuel Mix (RBF) and 25.5 µL Library Loading beads (LLB, ONT) and loaded into a R9.4 flowcell (ONT) via the SpotON port according to the manufacturer's instructions.

Nanopore sequencing data analysis. The Nanopore sequencing results were base called using the EPI2ME interface (v. 2.59.1896509). For passed 1D reads, quality scores (Q-score ≥ 7) and length distributions were evaluated using FastQC. Obtained fastq files were then converted to fasta files using the FASTX-toolkit (http://hannonlab.cshl.edu/fastx_toolkit/) and the sequences were aligned with the HPV genome database using LAST, with default parameters. Non-HPV reads, HPV reads and HPV type information was obtained. The non-HPV reads were filtered based on length, with only sequences >1.2 Kb or <1.6 Kb retained. For the retained non-HPV reads, taxonomies were annotated using the Greengenes database in QIIME⁸¹, with a ≥90% similarity level required. To further compare the results and obtain more thorough specie annotation results, LAST aligner⁸² was used in conjunction with a subset of the Greengenes database^{83,84} and the NCBI database. The obtained data was then evaluated by constructing a phylogenetic tree based on full-length 16S rRNA sequences from species (reads ≥ 5) identified by using the NCBI database and based on 10 genera that were commonly identified using three different analysis methods. The phylogenetic tree was visualized using MEGA X (<https://www.megasoftware.net>).

Illumina sequencing data analysis. To analyze the Illumina sequencing quality, FastQC version 0.11.8 (<http://www.bioinformatics.babraham.ac.uk/projects/fastqc/>) was utilized, and then the sequence reads were merged using FLASH-1.2.11 (Fast Length Adjustment of Short Reads; <http://ccb.jhu.edu/software/FLASH/>)⁸⁵ with a minimum overlap of 10. QIIME was used to filter and cluster combined pairs, with a quality score < Q20 and read length < 265 bp. These high-quality reads were then clustered using pick_otus.py in QIIME, with the UCLUST greedy algorithm utilized at a 97% similarity threshold. Taxonomies were defined using the GreenGenes database in QIIME at a 90% similarity threshold.

Comparison of Illumina and Nanopore sequencing data. The sequencing data were compared using the R statistical package version 3.6.0 (<https://www.r-project.org>), and Spearman's rank correlation tests were performed using the vegan package. Heatmaps and Venn diagrams were generated using the ggplot2 package within R.

HPV integration site sequencing and analysis. Integrated HPV sequences were enriched using HPV probes (Integrated DNA Technology, IDT) and an Illumina sequencing library was constructed using a NEBNext® Ultra II™ DNA Library Prep kit for Illumina® (E7370L) with NEBNext® Multiplex Oligos for Illumina® (E6609L) as recommended by the manufacturer. HPVDetector was used for the integration site analysis as previously described⁸⁶.

Integration site verification using Sanger sequencing. Primers were designed using Primer Premier 5.0, with two fusion sites with a high detection frequency targeted to generate an amplicon fragment size of 200 ~ 300 bp. The forward primers were designed based on HPV sequences, and the reverse primers were designed based on human genome sequences. B primers and C primers are displayed in Supplementary Table S11.

Sequences were amplified using Phoenix™ Hot Start Taq DNA Polymerase (Enzymatics) in a PCR reaction mix containing 4 µL 5X Phoenix Hot Start Taq Reaction Buffer, 2 µL dNTPs (2.5 µM), 0.5 µL each of forward and reverse primer (10 µM), 0.2 µL Phoenix™ Hot Start Taq DNA Polymerase (500 U), 1 µL template DNA (10 ng), and 12.3 µL Nuclease-Free Water (not DEPC-treated), for a total volume of 20 µL. The PCR amplification conditions were as follows: 5 min at 95 °C; 35 cycles at 94 °C for 30 s, 60 °C for 60 s for annealing, and 72 °C for 60 s; and a final 72 °C for 1 min. PCR products were visualized via agarose gel electrophoresis and cleaned-up using AMPure XP beads (Beckman Coulter, Miami, FL, USA).

Data availability

The datasets and analyses generated during this study are available in the Genbank database repository (accession: PRJNA545852; <https://www.ncbi.nlm.nih.gov/genbank/>).

Received: 24 June 2019; Accepted: 21 November 2019;

Published online: 18 December 2019

References

- Lloyd-Price, J. *et al.* Strains, functions and dynamics in the expanded Human Microbiome Project. *Nature* **550**, 61 (2017).
- Maruvada, P., Leone, V., Kaplan, L. M. & Chang, E. B. The Human Microbiome and Obesity: Moving beyond Associations. *Cell Host & Microbe* **22**, 589–599 (2017).
- Knight, R. *et al.* The Microbiome and Human Biology. *Annual Review of Genomics & Human Genetics* **18**, annurev-genom-083115-022438 (2017).
- Kyrgiou, M., Mitra, A. & Moscicki, A. B. Does the vaginal microbiota play a role in the development of cervical cancer? *Transl Res* **179**, 168–182, <https://doi.org/10.1016/j.trsl.2016.07.004> (2017).
- Lee, Y. C. *et al.* Association Between Helicobacter pylori Eradication and Gastric Cancer Incidence: A Systematic Review and Meta-analysis. *Gastroenterology* **150**, 1113–1124.e1115 (2016).
- Kostic, A. D. *et al.* Genomic analysis identifies association of Fusobacterium with colorectal carcinoma. *Genome Research* **22**, 292–298 (2012).
- Audirac-Chalifour, A. *et al.* Cervical Microbiome and Cytokine Profile at Various Stages of Cervical Cancer: A Pilot Study. *PLoS One* **11**, e0153274, <https://doi.org/10.1371/journal.pone.0153274> (2016).
- Mitra, A. *et al.* Cervical intraepithelial neoplasia disease progression is associated with increased vaginal microbiome diversity. *Scientific reports* **5**, 16865, <https://doi.org/10.1038/srep16865> (2015).
- Gao, W., Weng, J., Gao, Y. & Chen, X. Comparison of the vaginal microbiota diversity of women with and without human papillomavirus infection: a cross-sectional study. *Bmc Infectious Diseases* **13**, 271–271 (2013).
- Arokiyaraj, S., Seo, S. S., Kwon, M., Lee, J. K. & Kim, M. K. Association of cervical microbial community with persistence, clearance and negativity of Human Papillomavirus in Korean women: a longitudinal study. *Scientific reports* **8** (2018).
- Schelhaas, M. Viruses and cancer: molecular relations and perspectives. *Biological Chemistry* **398**, 815–816 (2017).
- Biswas, A. Human papillomavirus (HPV) and cervical cancer. *Journal of the Indian Medical Association* **98**, 53–55 (2000).
- Rebolj, M. *et al.* Primary cervical screening with high risk human papillomavirus testing: observational study. *BMJ* **364**, l240 (2019).
- Huang, J. *et al.* Comprehensive genomic variation profiling of cervical intraepithelial neoplasia and cervical cancer identifies potential targets for cervical cancer early warning. *Journal of medical genetics* **56**, 186–194, <https://doi.org/10.1136/jmedgenet-2018-105745> (2019).
- Goodman, A. HPV testing as a screen for cervical cancer. *Bmj* **350**, h2372 (2015).
- Ostade, X. V., Dom, M., Tjalma, W. & Raemdonck, G. V. Candidate biomarkers in the cervical vaginal fluid for the (self-)diagnosis of cervical precancer. *Archives of Gynecology & Obstetrics* **297**, 295–311 (2018).
- Oh, H. Y. *et al.* The association of uterine cervical microbiota with an increased risk for cervical intraepithelial neoplasia in Korea. *Clin Microbiol Infect* **21**(674), e671–679, <https://doi.org/10.1016/j.cmi.2015.02.026> (2015).
- Amabebe, E. & Anumba, D. O. C. The Vaginal Microenvironment: The Physiologic Role of Lactobacilli. *Front Med (Lausanne)* **5**, 181, <https://doi.org/10.3389/fmed.2018.00181> (2018).
- Vriend, H. J. *et al.* Incidence and persistence of carcinogenic genital human papillomavirus infections in young women with or without Chlamydia trachomatis infection. *Cancer Medicine* **4**, 1589–1598 (2015).

20. Wessels, J. M. *et al.* Association of high-risk sexual behaviour with diversity of the vaginal microbiota and abundance of *Lactobacillus*. *Plos One* **12**, e0187612 (2017).
21. Macklaim, J. M. *et al.* Exploring a road map to counter misconceptions about the cervicovaginal microbiome and disease. *Reproductive Sciences* **19**, 1154 (2012).
22. Kwasniewski, W. *et al.* Microbiota dysbiosis is associated with HPV-induced cervical carcinogenesis. *Oncol Lett* **16**, 7035–7047, <https://doi.org/10.3892/ol.2018.9509> (2018).
23. Davidson, R. M. & Epperson, L. E. Microbiome Sequencing Methods for Studying Human Diseases. *Methods Mol Biol* **1706**, 77–90 (2018).
24. Highlander, S. K. High throughput sequencing methods for microbiome profiling: application to food animal systems. *Animal Health Research Reviews* **13**, 40–53 (2012).
25. Alcon-Giner, C. *et al.* Optimisation of 16S rRNA gut microbiota profiling of extremely low birth weight infants. *Bmc Genomics* **18**, 841 (2017).
26. Anna, K. *et al.* Evaluation of general 16S ribosomal RNA gene PCR primers for classical and next-generation sequencing-based diversity studies. *Nucleic Acids Research* **41**, e1 (2012).
27. Fadrosch, D. W. *et al.* An improved dual-indexing approach for multiplexed 16S rRNA gene sequencing on the Illumina MiSeq platform. *Microbiome* **2**, 6–6 (2014).
28. Muinck, E. J. D., Trosvik, P., Gilfillan, G. D., Hov, J. R. & Sundaram, A. Y. M. A novel ultra high-throughput 16S rRNA gene amplicon sequencing library preparation method for the Illumina HiSeq platform. *Microbiome* **5**, 68 (2017).
29. Chakravorty, S., Helb, D., Burday, M., Connell, N. & Alland, D. A detailed analysis of 16S ribosomal RNA gene segments for the diagnosis of pathogenic bacteria. *Journal of Microbiological Methods* **69**, 330–339 (2007).
30. Zhang, J. *et al.* Evaluation of different 16S rRNA gene V regions for exploring bacterial diversity in a eutrophic freshwater lake. *Science of the Total Environment* **618** (2017).
31. Goodwin, S., Mcpherson, J. D. & McCombie, W. R. Coming of age: ten years of next-generation sequencing technologies. *Nature Reviews Genetics* **17**, 333–351 (2016).
32. Yang, B., Wang, Y. & Qian, P. Y. Sensitivity and correlation of hypervariable regions in 16S rRNA genes in phylogenetic analysis. *Bmc Bioinformatics* **17**, 135 (2016).
33. Payne, A., Holmes, N., Rakyan, V. & Loose, M. BulkVis: a graphical viewer for Oxford nanopore bulk FAST5 files. *Bioinformatics*, <https://doi.org/10.1093/bioinformatics/bty841> (2018).
34. Wagner, J. *et al.* Evaluation of PacBio sequencing for full-length bacterial 16S rRNA gene classification. *Bmc Microbiology* **16**, 274 (2016).
35. Shin, J. *et al.* Analysis of the mouse gut microbiome using full-length 16S rRNA amplicon sequencing. *Scientific reports* **6**, 29681 (2016).
36. Loman, N. J., Quick, J. & Simpson, J. T. A complete bacterial genome assembled de novo using only nanopore sequencing data. *Nature Methods* **12**, 733–735 (2015).
37. Lemon, J. K., Khil, P. P., Frank, K. M. & Dekker, J. P. Rapid Nanopore Sequencing of Plasmids and Resistance Gene Detection in Clinical Isolates. *Journal of clinical microbiology* **55**, JCM.01069-01017 (2017).
38. Merker, J. D. *et al.* Long-read genome sequencing identifies causal structural variation in a Mendelian disease. *Genetics in Medicine Official Journal of the American College of Medical Genetics* **20** (2017).
39. Quick, J. *et al.* Multiplex PCR method for MinION and Illumina sequencing of Zika and other virus genomes directly from clinical samples. *Nature Protocols* **12**, 1261 (2017).
40. Gong, L. *et al.* Culture-independent analysis of liver abscess using nanopore sequencing. *Plos One* **13**, e0190853 (2018).
41. Kilianski, A. *et al.* Bacterial and viral identification and differentiation by amplicon sequencing on the MinION nanopore sequencer. *GigaScience*, *4*, 1(2015-03-26) **4**, 12 (2015).
42. Benítez-Páez, A., Portune, K. J. & Sanz, Y. Species-level resolution of 16S rRNA gene amplicons sequenced through the MinION™ portable nanopore sequencer. *GigaScience*, *5*, 1(2016-01-28) **5**, 4 (2016).
43. Calus, S. T., Ijaz, U. Z. & Pinto, A. J. NanoAmpli-Seq: a workflow for amplicon sequencing for mixed microbial communities on the nanopore sequencing platform. *GigaScience* **7**, <https://doi.org/10.1093/gigascience/giy140> (2018).
44. Senapati, R., Senapati, N. N. & Dwivedi, B. Molecular mechanisms of HPV mediated neoplastic progression. *Infectious Agents & Cancer* **11**, 59 (2016).
45. Mineo, C. *Advances in Experimental Medicine and Biology* (2015).
46. Schwabe, R. F. & Jobin, C. The microbiome and cancer. *Nature Reviews Cancer* **13**, 800–812 (2013).
47. Chen, J., Domingue, J. C. & Sears, C. L. Microbiota dysbiosis in select human cancers: Evidence of association and causality. *Seminars in Immunology* **32**, 25 (2017).
48. Rui, M. F. *et al.* Gastric microbial community profiling reveals a dysbiotic cancer-associated microbiota. *Gut* **67**, gutjnl-2017-314205 (2017).
49. Moreau, M. M., Eades, S. C., Reinemeyer, C. R., Fugaro, M. N. & Onishi, J. C. Illumina sequencing of the V4 hypervariable region 16S rRNA gene reveals extensive changes in bacterial communities in the cecum following carbohydrate oral infusion and development of early-stage acute laminitis in the horse. *Veterinary microbiology* **168**, 436–441 (2014).
50. Brown, B. L., Watson, M., Minot, S. S., Rivera, M. C. & Franklin, R. B. MinION™ nanopore sequencing of environmental metagenomes: a synthetic approach. *Gigascience* **6**, 1–10 (2017).
51. Kerkhof, L. J., Dillon, K. P., Häggblom, M. M. & McGuinness, L. R. Profiling bacterial communities by MinION sequencing of ribosomal operons. *Microbiome* **5**, 116 (2017).
52. Kai, S. *et al.* Rapid bacterial identification by direct PCR amplification of 16S rRNA genes using the MinION nanopore sequencer. *FEBS open bio* **9**, 548–557, <https://doi.org/10.1002/2211-5463.12590> (2019).
53. Butt, S. L. *et al.* Rapid virulence prediction and identification of Newcastle disease virus genotypes using third-generation sequencing. *Virology Journal* **15**, 179, <https://doi.org/10.1186/s12985-018-1077-5> (2018).
54. Mitsuhashi, S. *et al.* A portable system for rapid bacterial composition analysis using a nanopore-based sequencer and laptop computer. *Scientific reports* **7**, 5657 (2017).
55. Lu, H., Giordano, F. & Ning, Z. Oxford Nanopore MinION Sequencing and Genome Assembly. *Genomics Proteomics & Bioinformatics* **14**, 265–279 (2016).
56. Leggett, R. M. & Clark, M. D. A world of opportunities with nanopore sequencing. *Journal of Experimental Botany* **68** (2017).
57. Hu, Y. O. O. *et al.* Stationary and portable sequencing-based approaches for tracing wastewater contamination in urban stormwater systems. *Scientific reports* **8**, 11907 (2018).
58. Benítez-Páez, A. & Sanz, Y. Multi-locus and long amplicon sequencing approach to study microbial diversity at species level using the MinION™ portable nanopore sequencer. *Gigascience* **6**, 1–12 (2017).
59. Moon, J. *et al.* *Campylobacter fetus* meningitis confirmed by a 16S rRNA gene analysis using the MinION nanopore sequencer, South Korea, 2016. *Emerging Microbes & Infections* **6**, e94 (2017).
60. Shin, H. *et al.* Elucidation of the bacterial communities associated with the harmful microalgae *Alexandrium tamarense* and *Cochlodinium polykrikoides* using nanopore sequencing. *Scientific reports* **8**, 5323 (2018).
61. Koren, S. *et al.* Canu: scalable and accurate long-read assembly via adaptive k-mer weighting and repeat separation. *Genome Research* **27**, 722 (2017).

62. Xiao, C. L. *et al.* MECAT: fast mapping, error correction, and de novo assembly for single-molecule sequencing reads. *Nature Methods* **14** (2017).
63. Lim, A. *et al.* Nanopore ultra-long read sequencing technology for antimicrobial resistance detection in *Mannheimia haemolytica*. *J Microbiol Methods* **159**, 138–147, <https://doi.org/10.1016/j.mimet.2019.03.001> (2019).
64. Denny, L., Kuhn, L., Pollack, A., Wainwright, H. & Wright, T. C. Evaluation of alternative methods of cervical cancer screening for resource-poor settings. *Cancer* **89**, 826–833 (2015).
65. Singh, V. B. *et al.* Liquid-based cytology versus conventional cytology for evaluation of cervical Pap smears: Experience from the first 1000 split samples. *Indian J Pathol Microbiol* **58**, 17–21 (2015).
66. Pretorius, R. G. *et al.* Colposcopically directed biopsy, random cervical biopsy, and endocervical curettage in the diagnosis of cervical intraepithelial neoplasia II or worse *. *American Journal of Obstetrics & Gynecology* **191**, 430–434 (2004).
67. Clarke, M. A. A large, population-based study of age-related associations between vaginal pH and human papillomavirus infection. *Bmc Infectious Diseases* **12**, 33–33 (2012).
68. Champer, M. *et al.* The role of the vaginal microbiome in gynecological cancer: a review. *Bjog An International Journal of Obstetrics & Gynaecology* **125** (2017).
69. Liang, W. S. *et al.* Simultaneous characterization of somatic events and HPV-18 integration in a metastatic cervical carcinoma patient using DNA and RNA sequencing. *International journal of gynecological cancer: official journal of the International Gynecological Cancer Society* **24**, 329–338, <https://doi.org/10.1097/igc.0000000000000049> (2014).
70. Zheng, H. *et al.* Genome-wide profiling of HPV integration in cervical cancer identifies clustered genomic hot spots and a potential microhomology-mediated integration mechanism. *Nature Genetics* **47**, 158–163 (2015).
71. Krashias, G., Koptides, D. & Christodoulou, C. HPV prevalence and type distribution in Cypriot women with cervical cytological abnormalities. *Bmc Infectious Diseases* **17**, 346 (2017).
72. Mitra, A. *et al.* The vaginal microbiota, human papillomavirus infection and cervical intraepithelial neoplasia: what do we know and where are we going next? *Microbiome* **4**, 58 (2016).
73. Lee, J. E. *et al.* Association of the vaginal microbiota with human papillomavirus infection in a Korean twin cohort. *Plos One* **8**, e63514 (2013).
74. Papachristou, E. K. *et al.* The shotgun proteomic study of the human ThinPrep cervical smear using iTRAQ mass-tagging and 2D LC-FT-Orbitrap-MS: the detection of the human papillomavirus at the protein level. *Journal of Proteome Research* **12**, 2078–2089 (2013).
75. Moon, J. *et al.* Rapid diagnosis of bacterial meningitis by nanopore 16S amplicon sequencing: A pilot study. *International journal of medical microbiology: IJMM* **309**, 151338, <https://doi.org/10.1016/j.ijmm.2019.151338> (2019).
76. Oyervides-Muñoz, M. A. *et al.* Understanding the HPV integration and its progression to cervical cancer. *Infection Genetics & Evolution* **61**, S156713481830090X (2018).
77. Akagi, K. *et al.* Genome-wide analysis of HPV integration in human cancers reveals recurrent, focal genomic instability. *Genome Research* **24**, 185 (2014).
78. Liu, Y., Lu, Z., Xu, R. & Ke, Y. Comprehensive mapping of the human papillomavirus (HPV) DNA integration sites in cervical carcinomas by HPV capture technology. *Oncotarget* **7**, 5852–5864 (2016).
79. Gao, G. *et al.* Common fragile sites (CFS) and extremely large CFS genes are targets for human papillomavirus integrations and chromosome rearrangements in oropharyngeal squamous cell carcinoma. *Genes Chromosomes Cancer* **56**, 59–74 (2016).
80. Kozich, J. J., Westcott, S. L., Baxter, N. T., Highlander, S. K. & Schloss, P. D. Development of a dual-index sequencing strategy and curation pipeline for analyzing amplicon sequence data on the MiSeq Illumina sequencing platform. *Appl. Environ. Microbiol* **79**, 5112–5120 (2013).
81. Caporaso, J. G. *et al.* QIIME allows analysis of high-throughput community sequencing data. *Nature Methods* **7**, 335, <https://doi.org/10.1038/nmeth.f.303> <https://www.nature.com/articles/nmeth.f.303#supplementary-information> (2010).
82. Frith, M. C., Hamada, M. & Horton, P. Parameters for accurate genome alignment. *Bmc Bioinformatics* **11**, 80 (2010).
83. Desantis, T. Z. *et al.* Greengenes: Chimera-checked 16S rRNA gene database and workbenchcompatible in ARB. *Applied & Environmental Microbiology* **72**, 5069–5072 (2006).
84. McDonald, D. *et al.* An improved Greengenes taxonomy with explicit ranks for ecological and evolutionary analyses of bacteria and archaea. *Isme Journal* **6**, 610–618 (2012).
85. Tanja, M. & Salzberg, S. L. FLASH: fast length adjustment of short reads to improve genome assemblies. *Bioinformatics* **27**, 2957–2963 (2011).
86. Chandrani, P. *et al.* NGS-based approach to determine the presence of HPV and their sites of integration in human cancer genome. *British Journal of Cancer* **112**, 1958 (2015).

Acknowledgements

We sincerely appreciate the support provided by the patient and her family. We would also like to thank all our team members for critically reviewing this manuscript.

Author contributions

Geng Tian acquired the funding for this study. Bo Meng and Geng Tian conceptualized the study. Lili Quan and Yu Song obtained the samples, patient consent letters and ethical approval letter for this study. Wenjuan Yang and Jia Liu conducted the experimentation and collected the data. Bo Meng, Ruyi Dong and Jidong Lang analyzed most of the results, while Wenjuan Yang performed additional analyses. Bo Meng, Wenjuan Yang and Lanyou Chen wrote the initial draft of the manuscript and Ruyi Dong prepared Figures 1–3. Bo Meng, Geng Tian and Weiwei Wang revised the manuscript. All authors discussed the results and reviewed the manuscript.

Competing interests

The authors declare no competing interests.

Additional information

Supplementary information is available for this paper at <https://doi.org/10.1038/s41598-019-55843-y>.

Correspondence and requests for materials should be addressed to B.M. or G.T.

Reprints and permissions information is available at www.nature.com/reprints.

Publisher's note Springer Nature remains neutral with regard to jurisdictional claims in published maps and institutional affiliations.



Open Access This article is licensed under a Creative Commons Attribution 4.0 International License, which permits use, sharing, adaptation, distribution and reproduction in any medium or format, as long as you give appropriate credit to the original author(s) and the source, provide a link to the Creative Commons license, and indicate if changes were made. The images or other third party material in this article are included in the article's Creative Commons license, unless indicated otherwise in a credit line to the material. If material is not included in the article's Creative Commons license and your intended use is not permitted by statutory regulation or exceeds the permitted use, you will need to obtain permission directly from the copyright holder. To view a copy of this license, visit <http://creativecommons.org/licenses/by/4.0/>.

© The Author(s) 2019